

The defect density in amorphous silicon

By M. STUTZMANN

Max-Planck-Institut für Festkörperforschung,
Heisenbergstraße 1, D-7000 Stuttgart 80, F.R. Germany

[Received 12 December 1988 and accepted 17 January 1989]

ABSTRACT

The correlation between the density of dangling-bond defects and the slope of the Urbach tail in hydrogenated amorphous silicon is examined. It is shown that this correlation can be explained quantitatively by a spontaneous decay of the weakest bonding orbitals into non-bonding defects during deposition or annealing of a sample and that the same correlation holds for all types of disorder affecting the slope of the Urbach edge. The temperature dependence of the defect density as well as the creation of metastable defects are discussed, and quantitative expressions are derived which can be used to estimate the quality and the stability of a given sample on the basis of the slope of its Urbach tail alone. Possible ways for future improvement of the material are indicated.

§ 1. INTRODUCTION

Recently, structural defects in amorphous silicon (a-Si) have been the subject of revived interest because of two developments. Firstly, it has been proposed that the main electronic defect levels in this material are not due to undercoordinated silicon atoms (dangling bonds, Si_3) which are only bonded to three nearest neighbours but rather to overcoordinated atoms (floating bonds, Si_5) which form molecular orbitals with five nearest-neighbour atoms (Pantelides 1986). The second development has been the suggestion that the density of defect states in a-Si may actually be determined by thermal equilibration between different configurations within the amorphous network, which is thought to be mediated by the movement of hydrogen (Street, Kakalios and Hayes 1986, Bar-Yam, Adler and Joannopoulos 1986, Smith and Wagner 1987, Müller 1988).

Whereas the identification of the main defect state in a-Si is mostly of academic interest, an understanding of what determines the overall density of defects in this material is a problem with immediate consequences for nearly all commercial applications of hydrogenated a-Si (a-Si:H) as envisaged today. Consequently, the influence of thermal equilibrium on the overall defect density of a-Si is of interest for many material scientists wishing to optimize this material for use in electronic devices. The purpose of the present paper is to show that thermal defect equilibration, although present to a certain degree, is only of minor importance for the overall defect density in a-Si:H. Instead, it is suggested that, irrespective of deposition temperatures and post-deposition thermal treatment, the minimum obtainable deep-defect density in a-Si is connected with the density of tail states in a very simple and predictable way.

§ 2. BAND-TAIL STATES AND DEEP DEFECTS IN a-Si

A possible connection between band-tail states and deep defects in a-Si is not a particularly new idea. Experimentally, it was established several years ago that there exists a close correlation between the slope E_0 of the exponential absorption edge in a-Si (the 'Urbach tail') and the density of deep defects observed in subgap absorption spectroscopy (Jackson and Amer 1981). Also, conceptually it seems quite obvious that there should be some connection between the weak bonds of an amorphous network (i.e. the tail states) and the broken bonds (i.e. the deep defects); with increasing bonding disorder, the density of strained bonds increases, and a certain fraction of these strained bonds will 'break' and then appear as deep defects states.† In this sense, the idea that weak bonds are the precursors for dangling bonds is very straightforward and can be found throughout the literature on amorphous semiconductors. Surprisingly, quantitative aspects of such a connection between tail states and deep defects in amorphous semiconductors have been investigated only recently.

Thus, in 1982, Street proposed a simple model to explain the creation of additional dangling-bond defects in doped a-Si. This model was based on solid-state defect reactions involving dangling bonds, dopant atoms and the a-Si lattice, with the concentrations of the various structural species only determined by thermal equilibrium creation and annihilation rates (Street 1982). Triggered by further experimental evidence, the main ideas of Street's model have been generalized by different workers to what has now become the thermal equilibrium model of a-Si (Street *et al.* 1986, Bar-Yam *et al.* 1986, Smith and Wagner 1987, Müller 1988, Kelires and Tersoff 1988). The essence of this model is that the main features of the electronic density of states in the mobility gap of doped or undoped a-Si : H are determined by a thermal equilibration between shallow states (dopants and tails) and deep defects (dangling bonds) established at the growth temperature. Here, the question arises to what extent and under which conditions thermal equilibration can occur in a material such as a-Si which, by definition, is far away from its thermal equilibrium state (i.e. the crystal). Thus the papers mentioned above differ mainly in the number of states thought to participate in different equilibration processes, and details of the thermal equilibrium model usually vary for undoped compared with doped a-Si, a-Si : H compared with unhydrogenated a-Si, or a-Si deposited under extreme deposition conditions. Of particular importance in the various thermal equilibration models is the temperature T in relation to the effective glass-transition temperature T_g of the disordered network. The existence of a well defined glass-transition temperature T_g implies that, for temperatures $T > T_g$, a noticeable fraction of the configurational coordinates of the network can maintain a thermal equilibrium distribution between themselves whereas, for $T < T_g$, the network structure becomes independent of temperature, as almost all structural degrees of freedom are 'frozen in' owing to kinetic inhibition of structural transitions. For $T \approx T_g$, different configurations can be realized in the same sample, depending on the thermal history (e.g. quenching or slow cooling).

The concept of (at least partial) thermal equilibrium in an amorphous semiconductor may be contrasted by the idea of a rigid disordered network, whose

† Note that this picture implies that the main defect state is indeed the dangling bond and not an overcoordinated silicon atom.

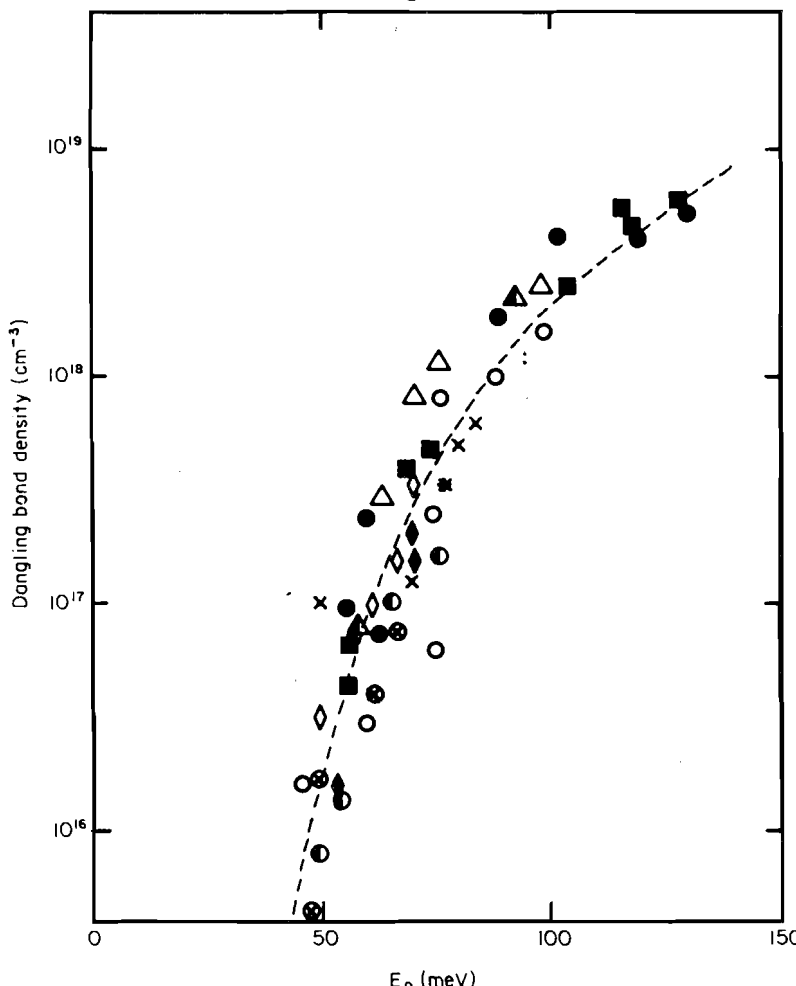
structure is essentially determined by local energy minimization during deposition or thermal annealing. Once the sample has been deposited at a temperature T_S (substrate temperature) or has been annealed at a temperature T_A , the structure of the sample is essentially independent of temperature for $T < T_S, T_A$, whereas changes in T_S or T_A lead to irreversible structural transitions. The idea behind this view of a disordered solid is that the minimum-energy configuration attainable by an amorphous network is determined predominantly by structural transitions occurring at the highest temperature in the thermal history of the solid. Once structural relaxation has been completed at this highest temperature, lower temperatures will not affect the network configuration to any significant amount.

Coming back to the special case of *a*-Si : H, it is now quite well established that the density of active dopants in this material may be described by a thermal equilibrium model (Street 1982, Street *et al.* 1986, Street, Hack and Jackson 1988). On the other hand, there is some doubt as to whether the main defect state in *a*-Si : H, namely the silicon dangling bond, is also involved in thermal equilibrium or not. Theoretically, it has been repeatedly suggested that dangling-bond defects in doped or undoped *a*-Si : H do equilibrate with shallow defect states such as dopants or band tails (Street 1982, Smith and Wagner 1987, Müller 1988). Experimentally, however, evidence for large-scale equilibration of dangling-bond defects is not entirely convincing. It is usually observed that the dangling-bond density for $T < T_S, T_A$ changes by a factor of only two or less (Smith, Aljishi, Slobodin, Chu, Wagner, Lenahan, Arya and Bennett 1986, Street *et al.* 1988, Xu, Okumura, Morimoto, Kumeda and Shimizu 1988), whereas changes in T_S or T_A can invoke changes of the dangling-bond density by up to four orders of magnitude. In view of the general remarks above, such a behaviour is more compatible with a rigid-network model for *a*-Si : H rather than with a thermal equilibration picture.

To proceed further, it is useful to assemble experimental evidence for a correlation between the dangling-bond defects in *a*-Si : H and shallow defect states for a large variety of different samples. This has been done in fig. 1, which shows the dangling-bond density obtained from subgap absorption measurements (photothermal deflection and constant photocurrent) as a function of the slope of the Urbach tail, given by $E_0(\alpha = \alpha_0 \exp[-(E - h\nu)/E_0]$ where α is the optical absorption coefficient), for about 50 *a*-Si : H specimens deposited in different reactors under different conditions, and also for different post-deposition treatments. Furthermore, the subgap absorption measurements have been performed by different groups, so that the data in fig. 1 should be quite representative for *a*-Si : H. In particular, the following experimental results are included in fig. 1:

- (1) undoped *a*-Si : H deposited under different conditions (open diamonds, open circles and crossed circles (Jackson and Amer 1981, 1982, Ley 1984));
- (2) undoped and doped (with phosphorus, arsenic or boron) *a*-Si : H with different doping levels deposited at substrate temperatures between 200 and 300 °C (crosses, half-filled triangles, full diamonds (M. Stutzmann 1988, unpublished));
- (3) *a*-Si : H with oxygen or nitrogen contamination (half-filled circles (Skumanich and Amer (1988));
- (4) lithium-diffused *a*-Si : H with different lithium concentrations (open triangles (K. Pierz and H. Mell 1988, private communication));
- (5) *n*-i-*p*-i superlattice (asterisks (M. Stutzmann 1988, unpublished));
- (6) undoped *a*-Si : H samples of different thicknesses, annealed up to 650 °C (filled circles and full squares (M. Ingels and M. Stutzmann 1988, unpublished)).

Fig. 1



Correlation between the dangling-bond defect density and the Urbach tail slope E_0 in a-Si:H. All data points were obtained from subgap absorption measurements. Symbols represent: (1) undoped a-Si:H (\diamond , \circ , \otimes); (2) undoped and doped a-Si:H deposited at 200–300°C (\times , Δ , \blacklozenge); (3) a-Si:H contaminated by O or N (\bullet); (4) Li-diffused a-Si:H (\triangle); (5) n–i–p–i superlattice (*); and (6) undoped a-Si:H annealed to 650°C (\blacksquare , \blacksquare). ---, fit to eqn. (2) with $N^* = 10^{21} \text{ cm}^{-3} \text{ eV}^{-1}$ and $E_{db} - E^* = 0.4 \text{ eV}$.

Given the usual experimental uncertainty (a factor of about two) for the determination of the defect density in a-Si:H, all data points in fig. 1 fall into a surprisingly narrow band, indicating a quite general relation between the midgap defect density and the Urbach tail slope E_0 . In particular, this correlation seems to be valid irrespective of substrate or annealing temperatures, doping levels, impurity contents, and so on. Thus, any explanation of this correlation has to involve a mechanism which is operative in a similar way for all the samples in fig. 1 and, especially, at very low and very high temperatures. The mechanism proposed in the following is based on an earlier article of the present author dealing with the structural transformation between weak bonds and dangling bonds in a-Si:H under non-equilibrium conditions (i.e.

during illumination, charge injection, or doping Stutzmann (1987)). The main idea behind the weak-bond dangling-bond conversion model is that a few (about 10^{20} cm^{-3} or less) extremely strained bonds in the *a*-Si network may be viewed as effective 'defect molecules' embedded in an otherwise rigid lattice. The bonding and antibonding levels of these defect molecules give rise to the localized tail states of the valence and the conduction band. Under non-equilibrium excitation conditions, excess charge carriers may be trapped in these defect molecules and cause them to dissociate, thereby leading to the formation of metastable dangling-bond defects (Stutzmann 1988).

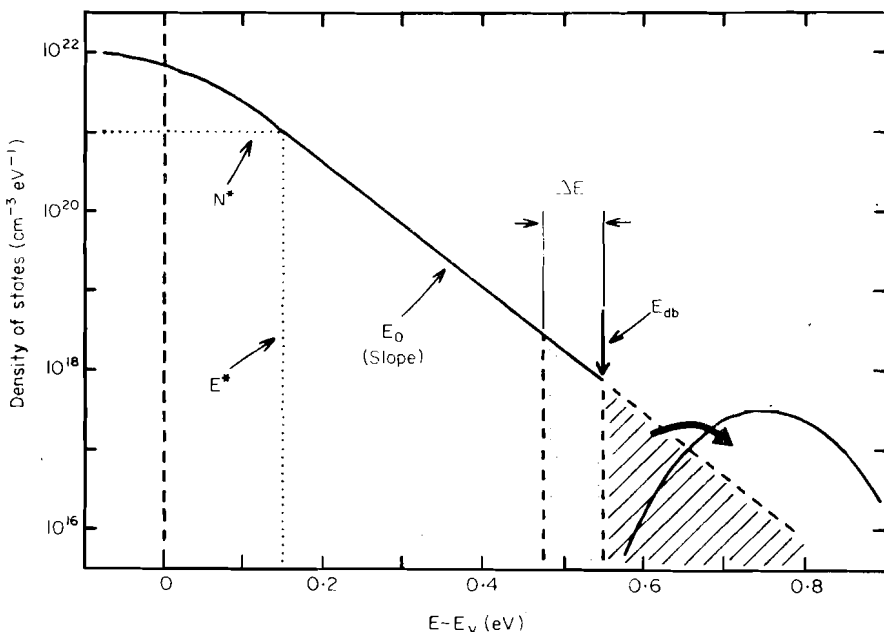
The same model can also be used to explain in a straightforward way the correlation between the defect density and the Urbach tail slope in fig. 1. To see this, consider the electronic density-of-states diagram shown in fig. 2, which depicts the energy region above the valence band mobility edge, $E_V = 0$. This energy region is mainly characterized by the exponential valence-band tail due to the bonding orbitals of weak Si-Si bonds. From optical absorption measurements as well as from recent photoemission measurements, it can be estimated that this exponential valence-band tail starts at an energy $E^* \approx E_V + 0.15 \text{ eV}$ with a density of states $N^* \approx 10^{21} \text{ cm}^{-3} \text{ eV}^{-1}$ (Jackson, Kelso, Tsai, Allen and Oh 1985, Winer, Hirabayashi and Ley 1988).

The exponential portion of the tail thus may be written as

$$N_{\text{tail}}(E) \approx N^* \exp [-(E - E^*)/E_0] \quad (1)$$

and comprises approximately 10^{18} – 10^{20} cm^{-3} weak bonds or 'defect molecules'. The exponential slope parameter E_0 in eqn. (1) can be directly observed as the Urbach tail slope parameter in the absorption spectra.

Fig. 2



Model for the density of states in *a*-Si:H above the valence-band mobility edge ($E_V = 0$): E_{db} denotes the demarcation energy above which valence-band tail states \square , decay spontaneously into dangling bonds; \square , tail states which can transform into metastable defects upon illumination, charge injection or weak doping.

Now, according to eqn. (1), the valence-band tail would extend indefinitely towards higher energies, which is, of course, an unphysical situation. This problem is resolved if we remember that the interatomic bonding potential becomes increasingly anharmonic for large deviations from the ideal (crystalline) bonding configuration. The effect of the anharmonicity is to concentrate bond strain on the weakest bonds rather than to distribute the strain equally on all bonds. The driving force for this disproportionation is the fact that the energy cost for increasing the strain at a weak bond is smaller than the energy gain due to the relaxation of the neighbouring 'back bonds'. This general property of an anharmonic bonding potential leads to a truncation of the exponential valence-band tail at a critical energy, E_{db} ; at this point, the additional energy necessary for breaking a weak bond is smaller than the energy gained by the relaxation of the surrounding network or, in other words, the weak bond dissociates spontaneously under the formation of two non-bonding states, that is dangling bonds. In the 'defect molecule' model, E_{db} is approximately the energy at which the bonding orbital of the strained molecule crosses the non-bonding atomic (sp^3) defect orbitals.

This spontaneous formation of dangling bonds in the disordered a-Si : H network is indicated in fig. 2; E_{db} denotes the demarcation energy beyond which valence-band tail states dissociate (shaded area). Note that the resulting dangling-bond defects may be slightly higher in energy than the unstable tail states with $E > E_{db}$, owing to the energy gained in the resulting lattice relaxation. The density of spontaneously formed dangling-bond defects can be obtained easily from eqn. (1) as

$$N_{db} \approx \int_{E_{db}}^{\infty} N_{tail} dE = N^* E_0 \exp\left(\frac{-(E_{db} - E^*)}{E_0}\right). \quad (2)$$

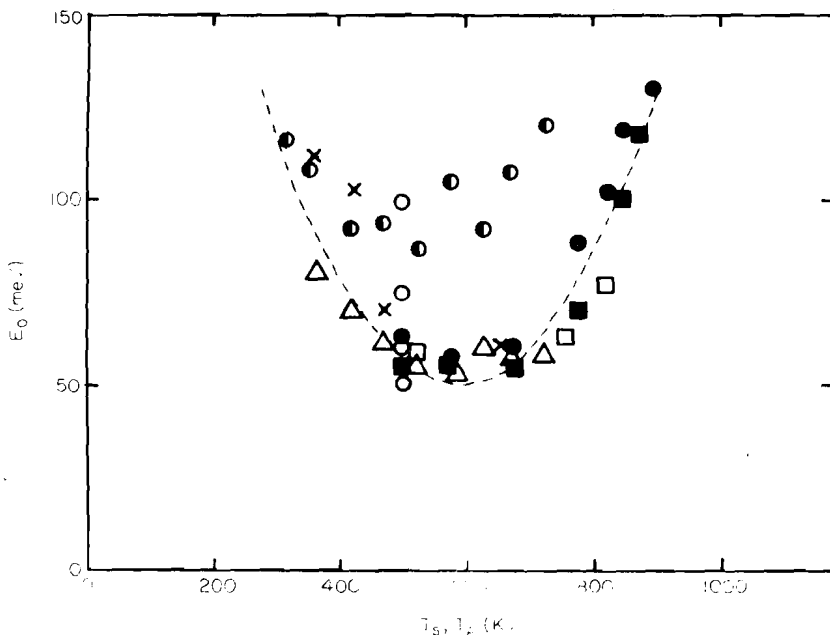
Equation (2) provides a simple general correlation between the defect density N_{db} and the Urbach tail slope E_0 in a-Si : H. The only free parameter in this relation, the demarcation energy E_{db} , can be obtained by fitting eqn. (2) to the experimental data in fig. 1. The broken line in fig. 1 shows a fit for $E_{db} - E^* = 0.4$ eV, or $E_{db} - E_v = 0.55$ eV. Typical error bars for this value are of the order of ± 50 meV. It is quite remarkable that this simple picture can provide an excellent quantitative fit to the experimental data in fig. 1. Moreover, the value obtained for E_{db} is in good agreement with estimates for the lower limit of the dangling-bond defect band in a-Si : H, as it should be according to the underlying physical picture; E_{db} should lie just at the crossing point of the valence-band tail and the defect band.

A relation identical with eqn. (2) has already been proposed by Smith and Wagner (1987) restricted, however, to a-Si : H samples deposited under non-optimal conditions (e.g. at low temperatures and high deposition rates). For optimized samples and especially for higher temperatures, Smith and Wagner deduced expressions for the dangling-bond density, which explicitly contained the temperature and a non-zero formation energy for dangling-bond defects. Smith and Wagner used these expressions to suggest that the dangling-bond density in undoped a-Si : H is determined by thermal equilibrium between tail states and defects. The main difference between the model of Smith and Wagner and the present picture of spontaneous weak-bond \rightarrow dangling-bond conversion concerns the role of temperature. In the thermal equilibration picture with a finite energy U for the formation of dangling-bond defects out of tail states, the defect density will involve a Boltzmann factor $\exp(-U/kT)$ for $T > T_g$, whereas for $T < T_g$ no explicit temperature dependence should occur, because of the freezing of the network structure at $T \approx T_g$. Thus the correlation between the band-tail slope E_0 and

the dangling-bond density should be strongly dependent on temperature, with a pronounced change at the glass-transition temperature T_g . In the weak-bond \rightarrow dangling-bond conversion model on the other hand, temperature plays only a secondary role; for a given band tail slope E_0 , the defect density will always be given to first order by eqn. (2), which does not contain the temperature as an explicit variable. The reason, of course, is that the conversion process as described in an earlier paper (Stutzmann 1987) is dominated by local transitions between nearly degenerate structures rather than by a global equilibration of the network.

It is already evident from fig. 1 that, as far as the role of temperature is concerned, the thermal equilibration model has some problems with the experimental evidence. The same relation between the dangling-bond defect density and the Urbach tail slope holds over a wide temperature range from room temperature up to the crystallization temperature. This would be incompatible with a Boltzmann factor $\exp(-U/kT)$, unless the formation energy U is close to zero, in which case the thermal equilibrium model would be equivalent to the weak-bond \rightarrow dangling-bond conversion model. Nevertheless, it is quite illuminating to introduce the (substrate or annealing) temperature again as an implicit variable in eqn. (2) and to study the temperature dependence of the Urbach tail slope E_0 and of the dangling-bond density N_{db} independently of each other. To this end, fig. 3 shows values of E_0 against temperature

Fig. 3



Dependence of the Urbach tail parameter E_0 on the substrate temperature T_S or annealing temperature T_A : ---, eqn. (3); \bullet , experimental data for undoped sputtered a-Si:H (Jousse, Bustarret and Boulitrop 1985); \times , experimental data for undoped glow-discharge a-Si:H (Kita, Yamagishi, Kamada, Okamoto and Hamakawa 1984); \triangle , experimental data for glow-discharge a-Si:H (Yamasaki 1987); \circ , experimental data for glow-discharge a-Si:H (Jackson and Amer 1982); \square , experimental data for glow-discharge a-Si:H (ref. 18 in the paper by Smith and Wagner (1987)); \blacksquare , \bullet , annealed glow-discharge a-Si:H (M. Ingels and M. Stutzmann 1988, unpublished).

for a variety of different samples. As far as possible, the data points in fig. 3 refer to samples not included in fig. 1, in order to avoid artificial correlations. It follows from fig. 3 that all data points for a-Si:H fall within a well defined part of the E_0 against (T_S, T_A) phase diagram, whose boundaries can be approximated by a simple parabola (broken curve in fig. 3):

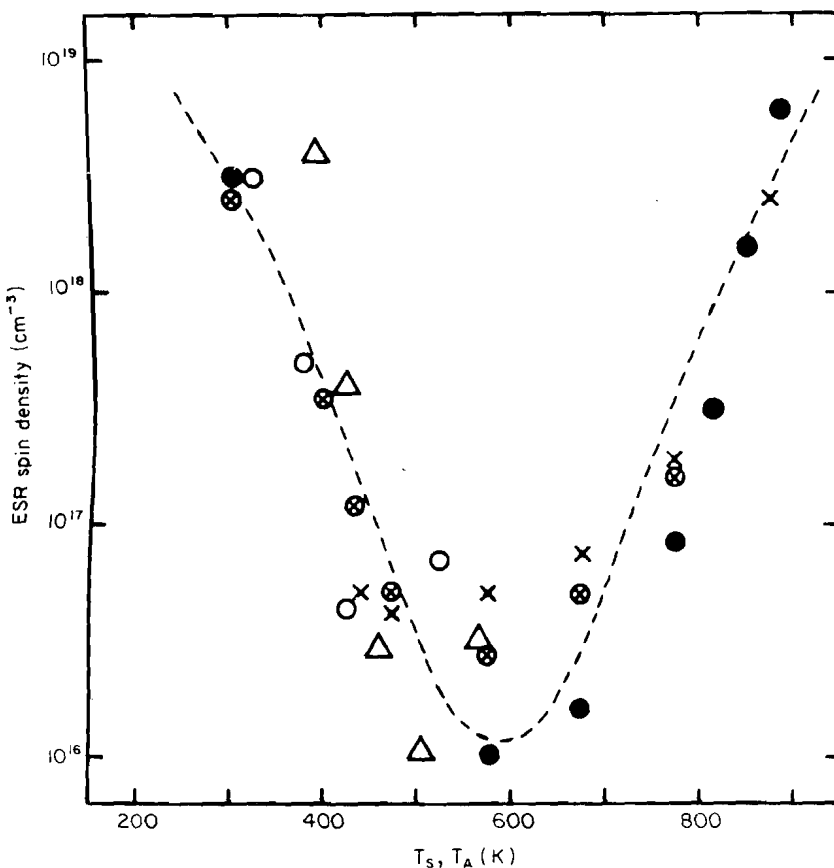
$$E_0 \gtrsim 50 \text{ meV} + 8.3 \times 10^{-4} (T - 590 \text{ K})^2 \text{ meV K}^{-2}. \quad (3)$$

Equation (3) constitutes the dependence of the Urbach tail slope on the substrate or annealing temperature mentioned above. As can be seen from fig. 3 or eqn. (3), the $E_0(T)$ dependence is quite symmetric for low and high temperatures, and the origin of this dependence is a very interesting point which will be discussed in somewhat more detail at the end of this paper. At present, however, we shall continue by presenting the counterpart of the $E_0(T)$ diagram in fig. 3, namely the temperature dependence of the dangling-bond density in undoped a-Si:H. Here, in order to prevent again unwanted artefacts for the resulting correlation between E_0 and N_{db} , we shall use the results of electron spin resonance (ESR) investigations, which provide values of $N_{db}(T)$ without knowledge of $E_0(T)$. In fig. 4, these ESR spin densities have been compiled as a function of substrate or annealing temperature. The desired connection with fig. 3 can now easily be made by extracting E_0 as a function of T from the broken line in fig. 3 (i.e. from eqn. (3)) and then calculating the ESR spin density via eqn. (2), under the assumption that $N_S \approx N_{db}$, that is all dangling-bond defects in undoped a-Si:H contribute to the $g=2.0055$ ESR resonance signal. Using this procedure, the broken curve in the $E_0(T)$ diagram transforms into the broken curve shown in the $N_S(T)$ diagram (fig. 4). The excellent agreement between the broken curve and the data points in fig. 4 then provides additional evidence for the fact that eqn. (2) indeed is valid for the entire temperature range. In particular, the same relation between E_0 and N_{db} is observed at room temperature, that is well below any glass-transition temperature at present discussed for a-Si:H, and at temperatures close to the crystallization point. This provides strong evidence for the fact that the correlation between E_0 and N_{db} as shown in fig. 1 is not the result of a thermal equilibration process but instead is established as a consequence of structural transitions which occur with similar probability independent of temperature.

§ 3. METASTABLE DEFECTS IN a-Si:H

Up to now, we have discussed only dangling-bond defects in a-Si:H which are formed spontaneously during the deposition of a-Si as a consequence of local energy minimization. These defects are characterized by the fact that their number can only be changed significantly in an irreversible way, namely by thermal annealing above the deposition temperature. On the other hand, it is well known that the dangling-bond density in high-quality a-Si can also be altered in a reversible manner by prolonged illumination (the 'Staebler-Wronski effect') or by irradiation with high-energy particles. Since these experimental conditions obviously deviate from a thermal equilibrium situation, the formation of metastable defects in a-Si:H cannot be described in the context of the thermal equilibration models mentioned above. The weak-bond \rightarrow dangling-bond conversion model, on the other hand, can provide a common description of both stable and metastable dangling-bond defects. Details concerning the formation of metastable defects have been discussed elsewhere (Stutzmann, Jackson and Tsai 1985, Stutzmann 1987) and will not be repeated here.

Fig. 4



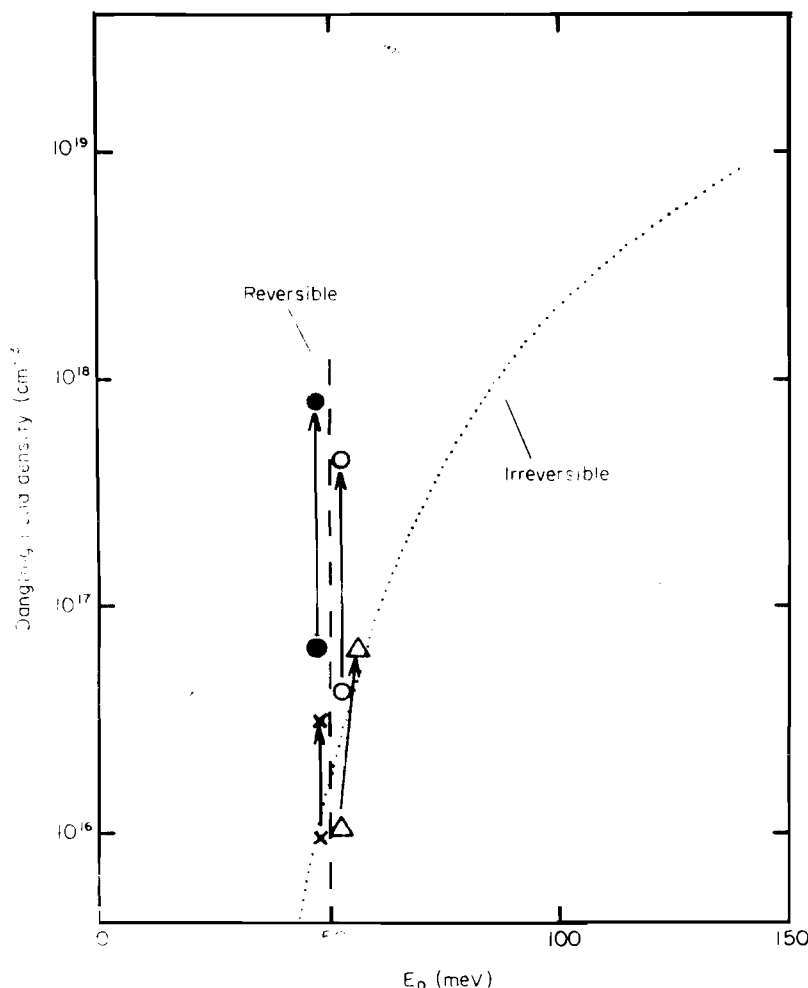
ESR spin density ($g = 2.0055$) in undoped $a\text{-Si:H}$ against substrate temperature T_S or annealing temperature T_A : ---, obtained from the broken line in fig. 3 via eqn. (2) as described in the text; ○, experimental data for sputtered $a\text{-Si:H}$ (Shimizu 1983); △, experimental data for glow-discharge $a\text{-Si:H}$ (Shirafuji, Kuwagaki, Sato and Inuishi 1984); ×, experimental data for annealed sputtered $a\text{-Si:H}$ (Wang, Li, Wei, Tang, Yan and Huang 1987); ○, experimental data for annealed glow-discharge $a\text{-Si:H}$ (Biegelsen, Street, Tsai and Knights 1979); ●, experimental data for annealed glow-discharge $a\text{-Si:H}$ (Stutzmann and Biegelsen 1983).

Instead, we shall concentrate on some quantitative aspects relating the Urbach tail slope E_0 and the density of metastable defects.

In order to understand the distinction between stable and metastable defects in $a\text{-Si:H}$, let us examine again fig. 2. Once an $a\text{-Si}$ film has been deposited under certain conditions, the distribution of bonding configurations is such that an exponential valence-band tail with a fixed slope E_0 exists. According to the weak-bond \rightarrow dangling-bond conversion scheme, all tail states beyond E_{db} have relaxed and formed dangling-bond defects. These defects are the stable defects of the network. If one now introduces an external excitation, such as intense light or energetic particles, it is possible to shift the demarcation energy E_{db} towards E_v by a small amount ΔE . Physically, this situation corresponds to the dissociation of tail states between E_{db} and $E_{db} - \Delta E$ into

additional metastable dangling bonds. The underlying process can be viewed as a mechanism which couples external excitation energy selectively into the deepest tail states (e.g. via charge carrier trapping or non-radiative recombination) and renders these tail states unstable. For the present purpose, it is sufficient to note that stable defects in a-Si : H are expected to follow eqn. (2), that is N_{db} increases as E_0 increases, whereas metastable dangling bonds should be formed without any significant change in E_0 , since only the fictitious demarcation energy E_{db} is shifted within a fixed band-tail density of states. Indeed, this is borne out by the experimental results. As shown in fig. 5,

Fig. 5



Dangling-bond density against Urbach tail slope E_0 for reversible defect creation in high-quality undoped a-Si : H: ··· correlation for stable defects according to fig. 1; Δ , experimental data, prolonged illumination (Wu, Qu and Han 1987); \times , experimental data, prolonged illumination (Amer, Skumanich and Jackson 1983); \circ , experimental data, electron-beam irradiation (Kazanskii, Korol, Milichevich and Chukichev 1986); \bullet , experimental data, electron-beam irradiation (Schneider, Schröder and Finger 1987).

metastable dangling bonds created by light soaking or electron irradiation tend to show a much smaller variation in E_0 with N_{db} as was observed for stable dangling bonds in fig. 2. In fact, in most cases, no increase in E_0 occurs experimentally, although N_{db} can increase reversibly by more than an order of magnitude.

According to the weak-bond \rightarrow dangling bond conversion model as suggested originally, a similar situation should also occur for the case of weak doping or single-carrier injection. Both situations are described by the fact that additional carriers are added to *a*-Si, which then occupy deep tail states and lead to a shift in the demarcation energy E_{db} either because electrons are taken out of bonding orbitals of weak bonds (p-type doping or hole injection), or because electrons are added to antibonding orbitals of weak bonds (n-type doping or electron injection) (Stutzmann 1987). Again, as in the case of illumination or irradiation, the overall effect can be envisaged as a shift of E_{db} in a material with constant E_0 , which will lead to formation of 'metastable' dangling bonds. (In the case of doping, however, this metastability cannot be seen, since the source of extra charge carriers, that is the active dopant atoms, cannot be removed without destroying the sample.) In this sense, the weak-bond \rightarrow dangling bond conversion model separates the creation of dangling bonds by doping into two components.

- (1) At low levels (e.g. 100 p.p.m. or less), doping does not affect the Urbach tail slope E_0 but rather the position of the demarcation energy E_{db} . In this regime, the increase in the dangling-bond density with doping can be related to the Fermi level position (which determines the fraction of doubly occupied and thus unstable tail states). These additional dangling bonds would be metastable if the dopants could be removed from the sample.
- (2) At high doping levels (about 500 p.p.m. or more, depending on the dopant), the incorporation of active or inactive dopant atoms also causes a noticeable broadening of the Urbach tail. Then new dangling bonds are created according to eqn. (2) even though the Fermi level and the demarcation energy E_{db} remain fixed. This is the case for the heavily doped films included in fig. 1.

Experimentally, both regime (1) and regime (2) have been observed in n-type *a*-Si : H doped with phosphorus or lithium (K. Pierz and H. Mell 1988, private communication).

Having defined the distinction between stable and metastable dangling-bond defects in *a*-Si : H, it is now interesting whether the underlying model can be used to evaluate the quality and the stability of a given *a*-Si sample quantitatively. Here, quality is related to the stable defect density N_{db} whereas reversible changes ΔN_{db} in this defect density are a measure of the material stability for many applications. In the context of the weak-bond \rightarrow dangling-bond conversion model, the most important figure of merit for an *a*-Si : H film then is the Urbach tail slope E_0 . Once E_0 is known, we can estimate the stable defect density, and therefore the quality of the film via eqn. (2). In the second step, following the discussion of metastable defects above, we can then express the stability of the film in terms of the shift ΔE of the demarcation energy E_{db} under light-soaking conditions (see fig. 2). From fig. 2, we obtain the defect density $N_{db}(B)$ in the light-soaked state as

$$N_{db}(B) = \int_{E_{db} - \Delta E}^{\infty} N_{tail} dE = \int_{E_{db} - \Delta E}^{E_{db}} N_{tail} dE + \int_{E_{db}}^{\infty} N_{tail} dE, \quad (4)$$

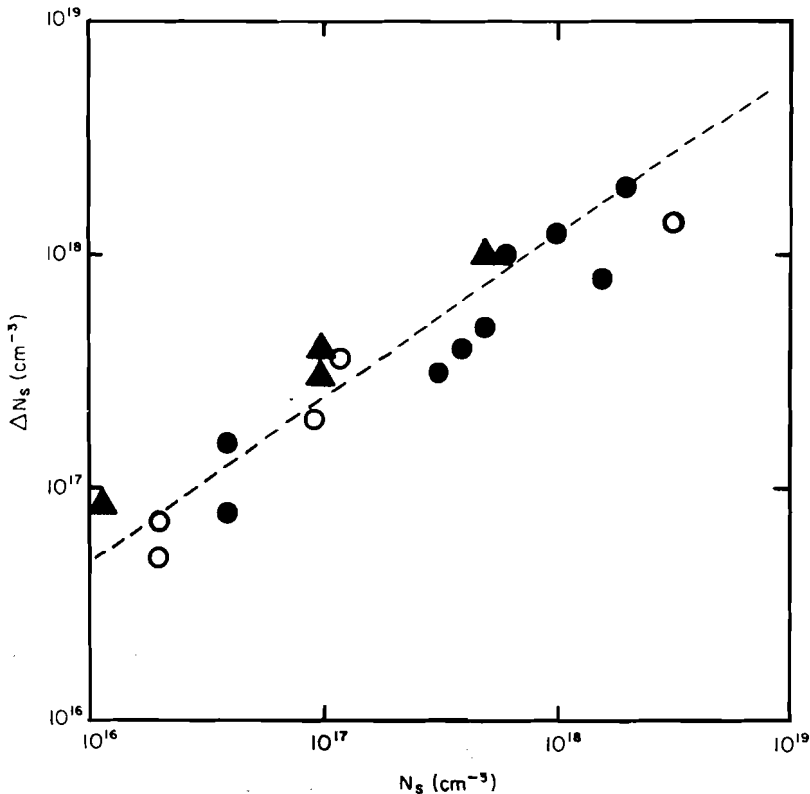
where the second term on the right-hand side is the stable defect density already known from eqn. (2), and the first term on the right-hand side constitutes the density ΔN_{db} of metastable defects. For this latter term a straightforward calculation yields

$$\Delta N_{db} = [\exp(\Delta E/E_0) - 1] N_{db}, \quad (5)$$

where the shift parameter ΔE is the only parameter necessary to quantify the sample stability. According to eqn. (5), there should be a close correlation between the stable defect density and the light-induced increase in the defect density, from which the shift parameter ΔE may be obtained. (Note that the slope constant E_0 in eqn. (5) is only an implicit variable which can be expressed through the defect density N_{db} via eqn. (2)!)

Experimentally, such a correlation between N_{db} and ΔN_{db} is indeed observed, as shown in fig. 6. The different data points in this figure refer to spin-density measurements of a-Si:H containing various amounts of impurities (full triangles (Stutzmann *et al.* 1985)), a-Si:H samples with different amounts of disorder produced by γ irradiation (full circles (Shirafuji, Shirakawa and Nagata 1986)) and a-Si:H films with different impurity and hydrogen contents produced by glow discharge and magnetron sputtering (open circles (Shimizu, Kumeda, Morimoto, Yokomichi and Ishii 1985)). The broken line in fig. 6 indicates a fit to eqn. (5) with $\Delta E \approx 80 \pm 10$ meV. Again it is quite remarkable that the experimental results for metastable defects in a wide range

Fig. 6



Correlation between the stable defect density N_s and the metastable defect density ΔN_s in undoped a-Si:H (see text for details):---, fit to eqn. (5) with $\Delta E = 80$ meV.

of a-Si:H samples can be explained quantitatively with only one parameter. This provides further support for the underlying model of local weak-bond \rightarrow dangling-bond conversion. For practical purposes, eqn. (5) expresses in a quantitative way what has already been known qualitatively about the light-induced degradation of a-Si:H, namely that good specimens degrade relatively more than bad samples. According to eqn. (5), the relative increase in the defect density is again a simple function of E_0 , if we assume $\Delta E \approx \text{constant} = 80 \text{ meV}$:

$$\Delta N/N \approx \exp(80 \text{ meV}/E_0) - 1. \quad (6)$$

Thus $\Delta N/N \approx 10$ for the best a-Si:H samples with $E_0 \approx 45 \text{ meV}$, whereas $\Delta N/N \approx 1$ for $E_0 \approx 100 \text{ meV}$, that is for samples with $N_{db} \approx 10^{18} \text{ cm}^{-3}$. For the degraded state after light soaking, we obtain from eqns. (2) and (4) (with $E_{db} - E^* \approx 0.4 \text{ eV}$ and $\Delta E \approx 0.08 \text{ eV}$)

$$N_{db}(B) \approx 10^{21} E_0 \exp(-0.3 \text{ eV}/E_0) \text{ cm}^{-1} \text{ eV}^{-1}, \quad (7)$$

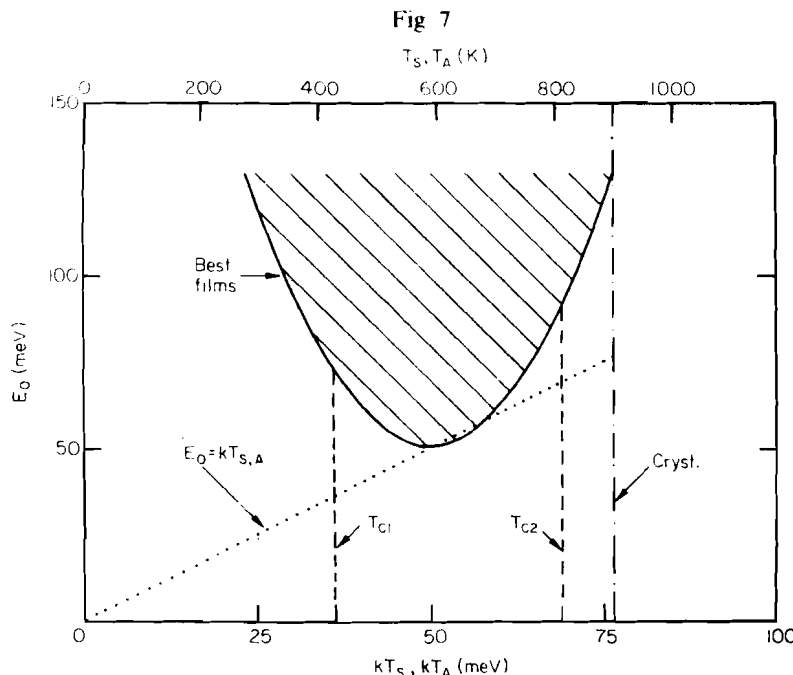
which shows that the key issue for the production of a-Si:H with good long-term quality is a reduction in the density of band-tail states contributing to E_0 .

§ 4. DEFECTS IN RELATED COVALENT SEMICONDUCTORS

We note in passing that the present description of the defect density can also be adapted quite easily to other covalent amorphous semiconductors such as hydrogenated amorphous germanium (a-Ge:H) or alloys of a-Si:H. All that is required is a knowledge of the Urbach tail slope E_0 and the energy position of the defect band of interest relative to the band which determines the Urbach tail. Then the defect density can again be estimated with the help of eqn. (2). To give an example, consider the case of a-Ge:H. In this material, it is known that the dangling-bond defect band is centred at about $E_V + 0.45 \text{ eV}$, that is much closer to E_V than in a-Si:H (Stutzmann, Stuke and Dersch 1983). Of course, this difference is due to the much smaller bandgap of a-Ge:H. Given the position of the dangling-bond band and a width of 0.2 eV f.w.h.m. as in a-Si:H, a reasonable estimate of the demarcation energy E_{db} in a-Ge:H would be $E_{db} \approx E_V + 0.35 \text{ eV}$. With $E^* \approx E_V + 0.15 \text{ eV}$ as in a-Si:H, we can then calculate from eqn. (2) a defect density N_{db} of about 10^{18} cm^{-3} for $E_0 = 60 \text{ meV}$, a value which is in good agreement with experimental results.

§ 5. LIMITATIONS OF THE URBACH TAIL SLOPE IN a-Si:H

To return to the case of pure a-Si:H, interesting questions are what limits the Urbach tail slope E_0 in this material and what could be done to reduce further this quantity and, thus, to improve the quality of a-Si:H films. For a discussion of this problem, it is useful to have a second look at the E_0 against T diagram (fig. 3). An idealized version of this diagram is shown in fig. 7. The shaded area again indicates the region of typical a-Si:H films available today, with the solid curve giving an approximation for $E_0(T_s, T_A)$ in the best films with a substrate temperature T_s or annealing temperature T_A (c.f. eqn. (3)). For higher temperatures, this phase diagram is limited by the crystallization temperature of about 900 K (chain line). Also indicated is the 'thermal disorder' path, $E_0 \approx kT_{s,A}$ (broken line). Along this path the valence-band tail slope is limited by the influence of thermal fluctuations of magnitude $\delta E \approx kT$ on the possible bonding configurations of a solid far from thermal equilibrium.



Schematic $E_0(T_s, T_4)$ phase diagram: \blacksquare , accessible region according to fig. 3; —, 'phase boundary' of a-Si:H with the lowest E_0 for a given temperature;, the condition $E_0 = kT_{s,A}$. T_{c1} and T_{c2} are the two critical temperatures described in the text.

The most remarkable point in fig. 7 is that $E_0 = kT_{s,A}$ appears to be a lower boundary for E_0 in a-Si. Moreover, this boundary is attained only in a small temperature range between 600 and 700 K (between about 300 and 400 °C). Since, according to eqn. (2) the lowest defect densities correspond to a minimal E_0 , a-Si:H films with the smallest stable defect densities are restricted to a narrow temperature interval around 300 °C. This explains phenomenologically why the substrate or annealing temperature is such an important parameter for the defect density in a-Si:H. In addition, from the fact that $E_0 \approx kT$, one can conclude that thermal equilibrium mechanisms may be important in the temperature range 200 °C $< T < 400$ °C, at least as far as band-tail states (or other shallow states such as dopants) are concerned. This is in general agreement with the experimental evidence.

Strong deviations from $E_0 \approx kT_{s,A}$ are evident for temperatures of 600 ± 200 K, labelled T_{c1} and T_{c2} in fig. 7. In fact, T_{c1} and T_{c2} as indicated have a microscopic meaning, which is related to the diffusion of hydrogen in a-Si:H. Hydrogen is the most mobile atom in a-Si:H (Carlson and Magee 1978, Beyer and Wagner 1982, Street, Tsai, Jackson and Kakalios 1987) and thus is generally considered to be responsible for structural changes in a-Si:H which occur below the crystallization temperature. Now, at $T_{c1} \approx 400$ K or below, the diffusion coefficient of hydrogen in a-Si:H is so small that every hydrogen atom will remain at its first bonding site encountered during deposition. Then the structure of the deposited a-Si:H film is essentially determined by a much larger effective temperature $T_{eff} \gg T_{s,A}$ characteristic for the glow-discharge plasma used for the film deposition. On the other hand, for $T \gtrsim T_{c2} \approx 800$ K, the

diffusion coefficient for hydrogen in a-Si is so large that most of the hydrogen will leave the a-Si sample during the deposition. In this case, E_0 will increase also, because the overall disorder in the a-Si network is then limited by much slower reconstruction processes based on the movement of silicon atoms, as fewer and fewer mobile hydrogen atoms are available for defect neutralization.

If, as suggested by fig. 7, the present limitation for the quality of a-Si:H is indeed the condition $E_0 \gtrsim kT_S$ together with the additional requirement for a sufficient density of mobile hydrogen atoms for defect neutralization, this would have obvious consequences for an improvement of a-Si:H film quality. Thus it would be necessary to decrease the substrate temperature to about 100°C in order to achieve a defect density of 10^{14} cm^{-3} ($E_0 \approx 35 \text{ meV}$). This temperature, however, is smaller than T_{C1} in fig. 7, meaning that hydrogen is essentially immobile under these conditions. Obviously, these two conflicting requirements can only be reconciled by more sophisticated methods of controlling the substrate temperature. For example, one could think of heating processes which couple excess energy selectively into the hydrogen-related modes, so that during deposition the hydrogen subsystem has a larger effective temperature than the a-Si network. In this way, it may be possible to decrease the average substrate temperature while still ensuring a sufficient mobility of hydrogen in the growth zone. This aspect of a-Si:H deposition should provide an interesting topic for future research.

§ 6. SUMMARY AND CONCLUSIONS

The main points of this paper can be summarized as follows.

- (1) Experimentally, one observes a strong correlation between the density of deep dangling-bond defects and the slope E_0 of the valence-band tail in a-Si:H. An increase in E_0 causes a well defined increase in the defect density. This correlation of the band-tail broadening is independent of the *origin* of the tail broadening (doping, impurity incorporation, too low or too high substrate or annealing temperatures, unfavourable deposition conditions).
- (2) The correlation between E_0 and the defect density can be described quantitatively by assuming that valence-band tail states above a cut-off energy $E_{db} \approx E_V + 0.55 \text{ eV}$ convert spontaneously into dangling-bond defects, either during the growth of the material or during annealing. This conversion is essentially irreversible and determines the minimum density of defects in a-Si. E_{db} corresponds to the cross-over between weak bond energies and the non-bonding defect levels, as suggested in the weak-bond \rightarrow dangling-bond conversion model.
- (3) Metastable defects, which can be created in a-Si:H by illumination, irradiation or charge injection, appear as a result of a reversible shift of the cut-off energy E_{db} towards the valence band. This causes an increase in the defect density without a corresponding increase in the band-tail slope E_0 . In the case of the Staebler-Wronski effect, a common value of $\Delta E \approx 80 \text{ meV}$ is obtained for the shift of E_{db} .
- (4) A survey of the band-tail slope parameter E_0 as a function of substrate or annealing temperature shows that all E_0 values fall within a well defined region of the $E_0(T)$ phase diagram. The minimum E_0 values coincide with $kT_{S,A}$, indicating that thermal disorder during deposition or annealing is the limiting factor for the quality of the best a-Si:H films.

(5) The observation that the same quantitative relation between the dangling bond density and the band tail slope is valid in the limits of very low and of very high temperatures indicates that thermal equilibration processes, which involve thermal creation of dangling bonds with a creation energy $U \gg kT$, are only of secondary importance for the dangling-bond density in *a*-Si : H. This does not exclude the possibility that thermal equilibration may be important for other types of defect (e.g. dopants).

ACKNOWLEDGMENTS

The author would like to thank W. Fuhs, H. Mell, K. Pierz and R. A. Street for helpful discussions.

REFERENCES

AMER, N. M., SKUMANICH, A., and JACKSON, W. B., 1983, *Physica B*, **117-118**, 897.
 BAR-YAM, Y., ADLER, D., and JOANNOPOULOS, J. D., 1986, *Phys. Rev. Lett.*, **57**, 467.
 BEYER, W., and WAGNER, H., 1982, *J. appl. Phys.*, **53**, 8745.
 BIEGELSEN, D. K., STREET, R. A., TSAI, C. C., and KNIGHTS, J. C., 1979, *Phys. Rev. B*, **20**, 4839.
 CARLSON, D. E., and MAGEE, C. W., 1978, *Appl. Phys. Lett.*, **33**, 81.
 JACKSON, W. B., and AMER, N. M., 1981, *J. Phys., Paris*, **42**, C4-293; 1982, *Phys. Rev. B*, **25**, 5559.
 JACKSON, W. B., KELSO, S. M., TSAI, C. C., ALLEN, J. W., and OH, S.-J., 1985, *Phys. Rev. B*, **31**, 5187.
 JOUSSE, D., BUSTARRET, E., and BOULITROP, F., 1985, *Solid State Commun.*, **55**, 435.
 KAZANSKII, A. G., KOROL, A. S., MILICHEVICH, E. P., and CHUKICHEV, M. V., 1986, *Sov. Phys.-Semicond.*, **20**, 1000.
 KELIRES, P. C., and TERSOFF, J., 1988, *Phys. Rev. Lett.*, **61**, 562.
 KITA, H., YAMAGISHI, H., KAMADA, T., OKAMOTO, H., and HAMAKAWA, Y., 1984, *Proceedings of the First International Photovoltaic Science and Engineering Conference*, edited by M. Konagai (Tokyo) p. 417.
 LEY, L., 1984, *The Physics of Hydrogenated Amorphous Silicon*, Vol. II, edited by I. D. Joannopoulos and G. Lucovsky (Berlin: Springer), p. 61.
 MÜLLER, G., 1988, *Appl. Phys. A*, **45**, 103.
 PANTELIDES, S. T., 1986, *Phys. Rev. Lett.*, **57**, 2979.
 SCHNEIDER, U., SCHRÖDER, B., and FINGER, F., 1987, *J. non-crystalline Solids*, **97-98**, 795.
 SHIMIZU, T., 1983, *J. non-crystalline Solids*, **59-60**, 117.
 SHIMIZU, T., KUMEDA, M., MORIMOTO, A., YOKOMICHI, H., and ISHII, N., 1985, *J. non-crystalline Solids*, **77-8**, 377.
 SHIRAFUJI, J., KUWAGAKI, M., SATO, T., and INUISHI, Y., 1984, *Jap. J. appl. Phys.*, **23**, 1278.
 SHIRAFUJI, J., SHIRAKAWA, K., and NAGATA, S., 1986, *Jap. J. appl. Phys.*, **25**, L634.
 SKUMANICH, A., and AMER, N. M., 1988, *Phys. Rev. B*, **37**, 8465.
 SMITH, Z. E., ALJISHI, S., SLOBODIN, D., CHU, V., WAGNER, S., LENAHAN, P. M., ARYA, R. R., and BENNETT, M. S., 1986, *Phys. Rev. Lett.*, **57**, 2450.
 SMITH, Z. E., and WAGNER, S., 1987, *Phys. Rev. Lett.*, **59**, 688.
 STREET, R. A., 1982, *Phys. Rev. Lett.*, **49**, 1187.
 STREET, R. A., HACK, M., and JACKSON, W. B., 1988, *Phys. Rev. B*, **37**, 4209.
 STREET, R. A., KAKALIOS, J., and HAYES, T. M., 1986, *Phys. Rev. B*, **34**, 3030.
 STREET, R. A., TSAI, C. C., JACKSON, W. B., and KAKALIOS, J., 1987, *Phil. Mag. B*, **56**, 305.
 STUTZMANN, M., 1987, *Phil. Mag. B*, **56**, 63; 1988, *Adv. Solid St. Phys.*, **28**, 1.
 STUTZMANN, M., and BIEGELSEN, D. K., 1983, *Phys. Rev. B*, **28**, 6256.
 STUTZMANN, M., JACKSON, W. B., and TSAI, C. C., 1985, *Phys. Rev. B*, **32**, 23.
 STUTZMANN, M., STUKE, J., and DERSCH, H., 1983, *Phys. Stat. sol. (b)*, **115**, 141.
 WANG, D., LI, Y., WEI, H., TANG, C., YAN, H., and HUANG, S., 1987, *J. non-crystalline Solids*, **95-96**, 841.
 WINER, K., HIRABAYASHI, I., and LEY, L., 1988, *Phys. Rev. B*, **38**, 7680.
 WU, W., QU, C., and HAN, D., 1987, *Proceedings of the International Workshop on Amorphous Semiconductors*, edited by H. Fritzsche, D.-X. Han and C. C. Tsai (Singapore: World Scientific), p. 181.
 XU, X., OKUMURA, A., MORIMOTO, A., KUMEDA, M., and SHIMIZU, T., 1988, *Phys. Rev. B*, **38**, 8371.
 YAMASAKI, S., 1987, *Phil. Mag. B*, **56**, 79.